NUMERICAL ANALYSIS OF HEAT AND MASS TRANSFER FROM A SPHERE WITH SURFACE MASS INJECTION OR SUCTION

PAILIN CHUCHOTTAWORN, AKIRA FUJINAMI AND KOICHI ASANO

Department of Chemical Engineering, Tokyo Institute of Technology, Tokyo 152

Key Words: Atomization, Mass Transfer, Heat Transfer, Numerical Analysis, Finite Difference Method, Sphere, High Mass Flux, Transfer Number

Numerical analyses for heat and mass transfer of a solid sphere without and with uniform, sinusoidal and evaporative mass injection or suction were made by use of a finite difference method for $Re_p = 1$–200, Pr or $Sc = 0.5$–2 and $\phi = -0.2$–0.5.

Numerical results for the case without mass injection or suction showed good agreement with the results of previous workers. Heat and mass transfer rates with uniform mass injection or suction were found to be affected by Re_p and Pr or Sc as well as mass injection ratio, ϕ.

New correlations for the effect of mass injection or suction on heat and mass transfer rates for the case with uniform and sinusoidal mass injection or suction in terms of transfer number were proposed. Heat and mass transfer rates with sinusoidal mass injection or suction showed good agreement with those for evaporative mass injection or suction.

Introduction

Heat and mass transfer from an evaporating liquid drop at high ambient temperatures is a fundamental problem in studies of spray drying, quenching and combustion of liquid fuel. Transport phenomena under such severe conditions are so complicated that under certain conditions surface mass efflux caused by evaporation will affect the velocity, temperature and concentration profiles. So heat and mass transfer of an evaporating liquid drop is quite different from that of a solid sphere.

Although many theoretical[1,3,7,10,16,17] and experimental[13–15] approaches to heat and mass transfer from an evaporating liquid drop have been made in past decades, most have studied the problem in a way similar to that for a solid sphere. A few approaches have been made in due consideration of the effect of surface mass efflux, which is essential to evaporation processes.[4,6,8,12,18]

In our previous papers,[2,5] we made a numerical approach to the effect of uniform mass injection or suction on the flow field around a solid sphere by a finite difference method. The purpose of the present study is to make an extensive numerical approach to heat and mass transfer under various conditions of surface mass injection or suction such as uniform, sinusoidal and evaporative mass injection or suction. Since calculation of evaporative mass injection requires very large computation time, major investigations were limited to the effect of uniform and sinusoidal mass injection or suction.

Received January 8, 1983. Correspondence concerning this article should be addressed to K. Asano. A. Fujinami is now at Asahi Glass Co., Ltd. Funabashi Plant, Chiba 273.

1. Method of Calculation

1.1 Governing equations

The Navier–Stokes equation for unsteady, incompressible, axisymmetric flow of constant properties in terms of stream function in spherical coordinates and the diffusion equation in terms of dimensionless concentration can be written as:

$$\frac{\partial}{\partial t}(E^2\psi)+\sin\theta\cdot\frac{\partial\psi}{\partial r}\cdot\frac{\partial}{\partial\theta}\left(\frac{E^2\psi}{r^2\sin^2\theta}\right)-\sin\theta\cdot\frac{\partial\psi}{\partial\theta}\cdot\frac{\partial}{\partial r}\left(\frac{E^2\psi}{r^2\sin^2\theta}\right)=\frac{2}{Re_p}E^2(E^2\psi) \quad (1)^*$$

where

$$E^2=\left(\frac{\partial^2}{\partial r^2}+\frac{\sin\theta}{r^2}\cdot\frac{\partial}{\partial\theta}\left(\frac{1}{\sin\theta}\cdot\frac{\partial}{\partial\theta}\right)\right) \quad (2)$$

and

$$\frac{(Re_p\cdot Sc)}{2}\left\{\frac{\partial\psi}{\partial r}\cdot\frac{\partial\theta_c}{\partial\theta}-\frac{\partial\psi}{\partial\theta}\cdot\frac{\partial\theta_c}{\partial r}\right\}$$

* Calculations of stream functions were made by use of the unsteady state equation of motion for ease of computation.[2,9]

$$=\sin\theta\left\{r^2\cdot\frac{\partial^2\theta_c}{\partial r^2}+2r\frac{\partial\theta_c}{\partial r}+\cot\theta\frac{\partial\theta_c}{\partial\theta}+\frac{\partial^2\theta_c}{\partial\theta^2}\right) \quad (3)^*$$

The boundary conditions for uniform mass injection or suction are:

$$\theta=0:\psi=0 \quad (4a)$$

$$\partial\theta_c/\partial\theta=0 \quad (4b)$$

$$\theta=\pi:\psi=-2\phi \quad (4c)$$

$$\partial\theta_c/\partial\theta=0 \quad (4d)$$

$$r=1:\psi=\phi(\cos\theta-1) \quad (4e)$$

$$\theta_c=0 \quad (4f)$$

$$r=r_\infty:\psi=\frac{1}{2}r_\infty{}^2\sin^2\theta+\phi(\cos\theta-1) \quad (4g)$$

$$\theta_c=1 \quad (4h)$$

where Eq. (4e) represents the condition of uniform mass injection or suction on the drop surface and ϕ $(=(u_r')_{r'=A}/U_\infty)$ is the mass injection ratio. The boundary conditions for the case with sinusoidal mass injection or suction are almost same as those for the case with uniform mass injection or suction except that Eqs. (4e) and (4g) are replaced by Eqs. (4i) and (4j) as:

$$r=1:\psi=\phi(\cos\theta-1)+\phi(\cos2\theta-1)/4 \quad (4i)$$

$$r=r_\infty:\psi=(r_\infty{}^2\sin^2\theta)/2+\phi(\cos\theta-1)+\phi(\cos2\theta-1)/4 \quad (4j)$$

1.2 Finite difference method

Equations (1) and (3) were solved successively by a finite difference method with relaxation technique. Since the stream function and the concentration change rapidly near the surface of the sphere, an exponential step size in the radial direction was used.[2)]

$$r=\exp(z) \quad (5)$$

We have already discussed the computation method for Eq. (1) in detail in our previous paper,[2)] so only the computation method for Eq. (3) will be discussed hereafter. Equation (3) can be rewritten as:

$$\frac{(Re_pSc)}{2}\left(\frac{\partial\psi}{\partial z}\cdot\frac{\partial\theta_c}{\partial\theta}-\frac{\partial\psi}{\partial\theta}\cdot\frac{\partial\theta_c}{\partial z}\right)=\exp(z)\cdot\sin\theta\left(\frac{\partial^2\theta_c}{\partial z^2}+\frac{\partial\theta_c}{\partial z}+\cot\theta\frac{\partial\theta_c}{\partial\theta}+\frac{\partial^2\theta_c}{\partial\theta^2}\right) \quad (6)$$

Equation (6) is transformed into a finite difference form by use of Taylor series expansion correct to the second-order term. The resulting finite difference form of Eq. (6) can be written as:

$$\theta^k_{c_{i,j}}=\left[\left\{\frac{1}{\Delta z^2}+\frac{1}{2\Delta z}+\frac{Re_pSc(\psi_{i,j+1}-\psi_{i,j-1})}{8\cdot\Delta z\cdot\Delta\theta\cdot\exp(z)\cdot\sin\theta}\right\}\theta^k_{c_{i+1,j}}+\left\{\frac{1}{\Delta z^2}-\frac{1}{2\Delta z}-\frac{Re_pSc(\psi_{i,j+1}-\psi_{i,j-1})}{8\cdot\Delta z\cdot\Delta\theta\cdot\exp(z)\cdot\sin\theta}\right\}\theta^k_{c_{i-1,j}}+\left\{\frac{1}{\Delta\theta^2}+\frac{\cot\theta}{2\Delta\theta}-\frac{Re_pSc(\psi_{i+1,j}-\psi_{i-1,j})}{8\cdot\Delta z\cdot\Delta\theta\cdot\exp(z)\cdot\sin\theta}\right\}\theta^k_{c_{i,j+1}}+\left\{\frac{1}{\Delta\theta^2}-\frac{\cot\theta}{2\Delta\theta}+\frac{Re_pSc(\psi_{i+1,j}-\psi_{i-1,j})}{8\cdot\Delta z\cdot\Delta\theta\cdot\exp(z)\cdot\sin\theta}\right\}\theta^k_{c_{i,j-1}}\right]\Big/2\left(\frac{1}{\Delta z^2}+\frac{1}{\Delta\theta^2}\right) \quad (7)$$

Equation (7) with boundary conditions of Eqs. (4a)–(4h) for uniform mass injection or suction, or (4a)–(4d), (4f), (4h), (4i) and (4j) for sinusoidal mass injection or suction were solved iteratively by a relaxation method. The circular mesh system employed in the present calculation was the same as that used in the previous paper.[2)]

The following convergence criteria were used for calculation of concentration profiles for the case with uniform and sinusoidal mass injection or suction:

$$\left|\frac{\theta_c{}^{k+1}-\theta_c{}^k}{\theta_c{}^{k+1}}\right|<10^{-4} \quad (8)$$

$$|\theta_c{}^{k+1}-\theta_c{}^k|<10^{-6} \quad (9)^*$$

1.3 Calculation of Nusselt and Sherwood numbers

Dimensionless local heat and diffusion fluxes were calculated from the temperature and concentration profiles by the following equations:

$$Nu_\theta\equiv\frac{2A\cdot q_\theta|_{r=1}}{\kappa\cdot(T_s-T_\infty)}=2\left(\frac{\partial\theta_t}{\partial r}\right)_{r=1} \quad (10)$$

$$Sh_\theta(1-\omega_s)\equiv\frac{2A\cdot N_{A\theta|r=1}}{\rho\mathscr{D}(\omega_s-\omega_\infty)}\cdot(1-\omega_s)=2\left(\frac{\partial\theta_c}{\partial r}\right)_{r=1} \quad (11)$$

The average heat and diffusion fluxes were calculated by:

$$Nu\equiv\frac{2A\cdot\bar{q}|_{r=1}}{\kappa\cdot(T_s-T_\infty)}=\int_0^\pi\left(\frac{\partial\theta_t}{\partial r}\right)_{r=1}\cdot\sin\theta\cdot d\theta \quad (12)$$

$$Sh(1-\omega_s)\equiv\frac{2A\cdot\bar{N}_{A|r=1}}{\rho\mathscr{D}(\omega_s-\omega_\infty)}\cdot(1-\omega_s)$$

* Since the governing equation and the boundary conditions are mathematically similar for heat and mass transfer, the results for mass transfer can be easily applied for heat transfer. For this reason the energy equation is not shown here.

* Values of the left-hand side of Eq. (8) will not converge as θ_c approaches zero, so an additional convergence criterion, Eq. (9), was also used.

Table 1. Ranges of variables of numerical analysis

Re_p	Pr or Sc	ϕ
Uniform mass injection and suction		
1	0.5–2.0	0–0.5
2	0.5–2.0	0–0.3
3	0.5–2.0	0–0.4
5	0.5–2.0	−0.1–0.2
10	0.5–2.0	−0.2–2.0
20	0.5–2.0	0–0.2
30	0.5–2.0	−0.2–0.15
50	0.5–2.0	−0.07–0.15
80	0.5–2.0	0–0.1
100	0.5–2.0	−0.05–0.04
150	0.5–2.0	−0.04–0.04
200	0.5–2.0	0
Cosine-curve mass injection and suction		
5	0.5–2.0	−0.1–0.2
10	0.5–2.0	−0.2–0.2
30	0.5–2.0	−0.2–0.15
50	0.5–2.0	−0.07–0.15
100	0.5–2.0	−0.05–0.04
150	0.5–2.0	−0.04–0.04
Evaporative mass injection and suction		
5	0.5–2.0	−0.11–0.11
50	0.5–2.0	−0.08–0.16
150	0.5–2.0	−0.05–0.03

$$= \int_0^{\pi} \left(\frac{\partial \theta_c}{\partial r}\right)_{r=1} \cdot \sin\theta \cdot d\theta \qquad (13)$$

Calculations were made with HITAC M-200H computer. The range of variables is shown in **Table 1**.

2. Numerical Results with and without Uniform Mass Injection or Suction

2.1 Comparison of numerical results for the case without mass injection or suction

To investigate the accuracy of the present method, the calculated average heat and diffusion fluxes were compared with the results of previous workers for the case without mass injection or suction.[1,14,17]

Figure 1 shows the result of the comparison at Pr or $Sc=0.75$, where the dotted line represents the Ranz–Marshall correlation[14]:

$$Sh_0(1-\omega_s) = 2 + 0.6 Re_p^{1/2} Sc^{1/3} \qquad (14)$$

and the dot-dash line represents the Brauer–Sucker correlation[1]:

$$Sh_0(1-\omega_s) = 2 + \frac{0.66(Re_p Sc)^{1.7}}{\{1+(Re_p Sc)^{1.2}\}\{1+(0.84 Sc^{1/6})^3\}^{1/3}} \qquad (15)$$

Good agreement between present and previous calculations is observed. The present calculations also show good agreement with the numerical data by Woo *et al.*[17]

The present numerical results of dimensionless

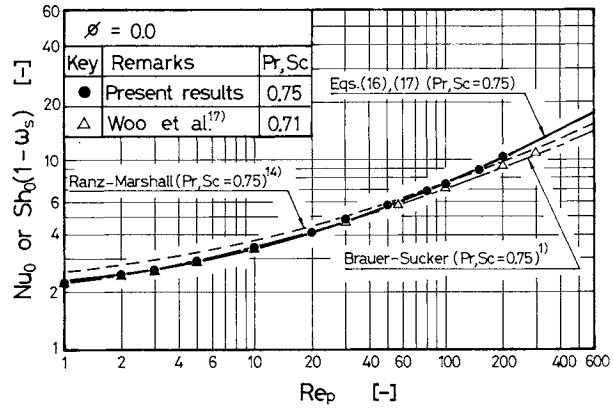

Fig. 1. Heat and mass transfer rates from a solid sphere without surface mass injection or suction.

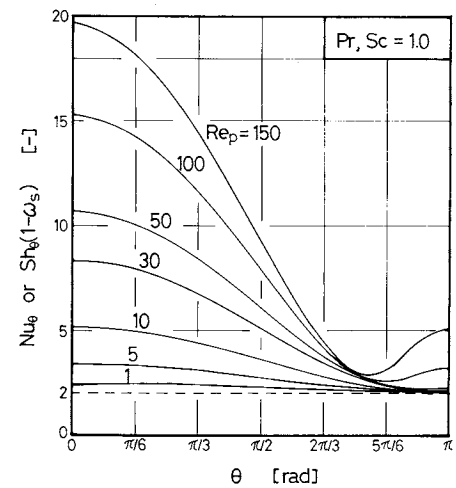

Fig. 2. Local distribution of heat and diffusion fluxes without surface mass injection or suction.

diffusion fluxes for the case without mass injection or suction are well correlated by:

$$Sh_0(1-\omega_s) = 2 + 0.37 \cdot Re_p^{0.61} \cdot Sc^{0.51} \qquad (16)$$

for $Re_p=1$–200 and $Sc=0.5$–2.0 with accuracy better than 2%. Similar correlation is obtained for Nusselt number as:

$$Nu_0 = 2 + 0.37 \cdot Re_p^{0.61} \cdot Pr^{0.51} \qquad (17)$$

The solid line in the figure represents Eqs. (16) and (17). In the discussion below, Eqs. (16) or (17) are used for correlation of the effect of finite mass flux.

Figure 2 shows the distribution of the local heat and diffusion fluxes without surface mass injection or suction at various Reynolds numbers ranging from 10 to 150 at Pr or $Sc=1$.

2.2 Effect of uniform mass injection or suction on heat and diffusion fluxes

For numerical analysis of the effect of mass injection or suction on the rates of heat and mass transfer from a solid sphere, distribution of the local mass flux over the surface of the sphere is necessary. Since no solution under such conditions is available at

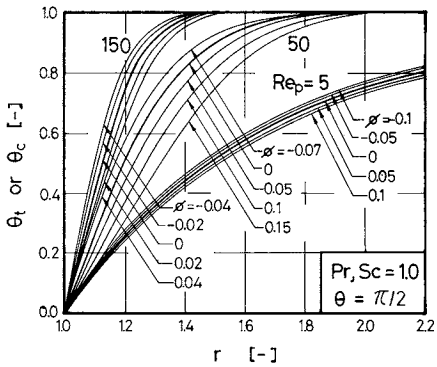

Fig. 3. Effect of uniform mass injection or suction on temperature or concentration profiles on equatorial plane of a sphere.

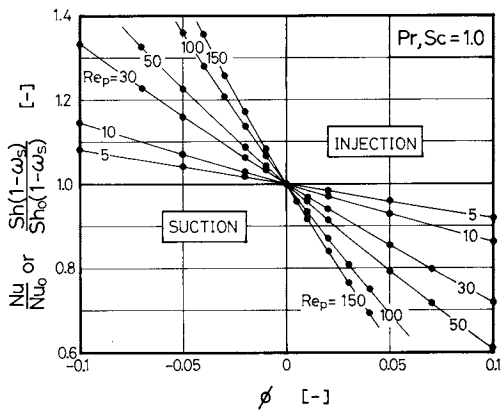

Fig. 4. Effect of uniform mass injection or suction on average heat and diffusion fluxes at various Reynolds numbers.

present which predicts local mass flux from an evaporating liquid drop, uniform mass injection or suction has been taken as a first approximation for obtaining a numerical solution,* according to the suggestion by Hoffman and Ross.[8)]

Figure 3 shows the effect of uniform mass injection or suction on temperature or concentration profiles on the equatorial plane ($\theta=\pi/2$) at various Reynolds numbers ranging from 5 to 150 and at Pr or $Sc=1$. The figure indicates that the thickness of the thermal and concentration boundary layer increases with increasing mass injection ratio, and that the effect of mass injection becomes considerable as Reynolds number increases.

Figure 4 shows the effect of uniform mass injection or suction on average Nusselt number or dimensionless diffusion flux at various Reynolds numbers ranging from 5 to 150 at Pr or $Sc=1$. The figure indicates that the effect is considerable as Reynolds number

* Figure 2 may indicate that assumption of uniform mass injection or suction is a fairly good approximation for the Reynolds number range which is of practical importance for combustion of liquid fuel.

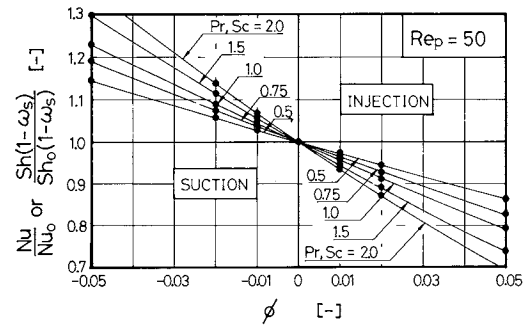

Fig. 5. Effect of uniform mass injection or suction on average heat and diffusion fluxes at various Prandtl or Schmidt numbers.

increases. This may be due to the change of boundary layer thickness shown in Fig. 3.

Figure 5 shows the effect of mass injection or suction on average Nusselt numbers or dimensionless diffusion fluxes at various Prandtl or Schmidt numbers ranging from 0.5 to 2 at $Re_p=50$. The figure indicates that the effect is considerable as Prandtl or Schmidt number increases.

2.3 Correlation of numerical data with uniform mass injection or suction

The discussion in the previous section may indicate that the rates of heat and mass transfer with mass injection or suction are a complicated function of Re_p, Pr or Sc and ϕ as:

$$Nu/Nu_0=g(Re_p, Pr, \phi) \tag{18}$$

$$Sh(1-\omega_s)/Sh_0(1-\omega_s)=g(Re_p, Sc, \phi) \tag{19}$$

Hoffman and Ross[8)] suggested use of the Spalding transfer number or transfer number for heat transfer, B_H, defined as:

$$B_H=Re_p\cdot\phi\cdot Pr/Nu \tag{20}*$$

for correlation of heat transfer data. This may suggest use of the transfer number for mass transfer, B_M, defined as:

$$B_M=Re_p\cdot\phi\cdot Sc/Sh(1-\omega_s) \tag{21}*$$

for correlation of mass transfer data.

Figure 6 shows the results of correlation. All the data by the present calculation are well correlated by:

$$g(B)=1/\{0.3+0.7(1+B)^{0.75}\} \tag{22}$$

$$-0.78\leq B\leq 7.4$$

($B=B_H$ for heat transfer;
$B=B_M$ for mass transfer)

with maximum deviation less than 3%. **Figure 7** shows

* For the case with nonuniform mass injection or suction (Sections 3.1 and 3.2), ϕ is taken as the average over the surface of the sphere.

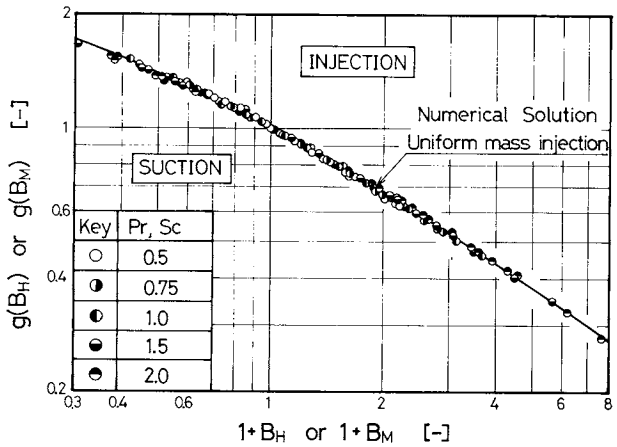

Fig. 6. Correlation of the effect of uniform mass injection or suction on average heat and diffusion fluxes.

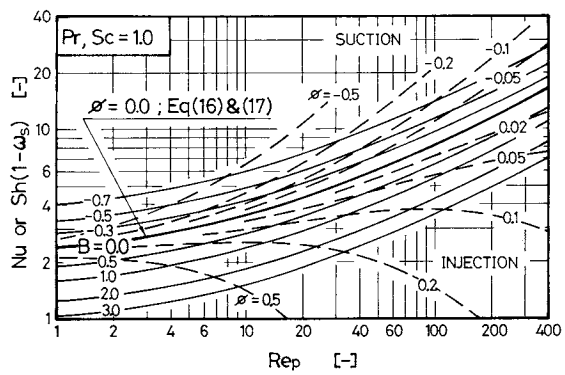

Fig. 7. Effect of mass injection ratio and of transfer number on average heat and diffusion fluxes for the case with uniform mass injection or suction.

the effect of mass injection ratio and transfer number on heat and diffusion fluxes.

3. Numerical Results with Nonuniform Mass Injection or Suction

3.1 Sinusoidal mass injection or suction

We have assumed uniform mass injection as a first approximation to evaporation of a liquid drop, but calculation of heat and diffusion fluxes without mass injection (cf. Fig. 2) suggests another type of mass injection as a second approximation. Cosine-curve mass injection or suction given by:

$$(u_r)_{r=1} = \phi(1+\cos\theta) \tag{23}$$

was chosen for this purpose, and from it the boundary condition Eq. (4i) was given.

Calculation was carried out in a similar way to that for uniform mass injection or suction. As was the case with uniform mass injection or suction, all the numerical data for the case with cosine-curve mass injection or suction were well correlated by the following equation:

$$g(B) = 1/\{0.3+0.7(1+B)^{0.88}\} \tag{24}$$

$$(-0.65 \leqq B \leqq 4.9)$$

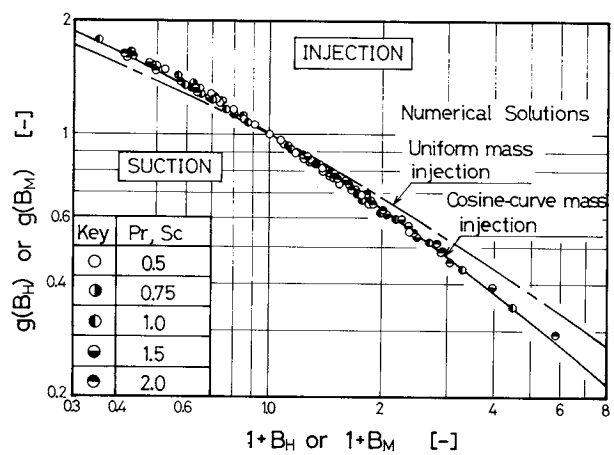

Fig. 8. Correlation of the effect of cosine-curve mass injection or suction on average heat and diffusion fluxes.

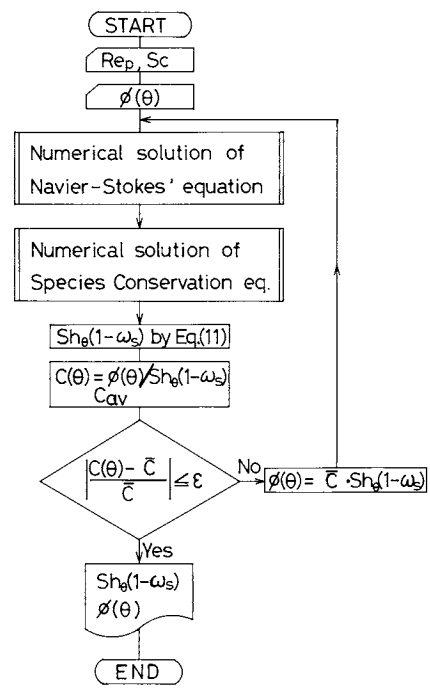

Fig. 9. Flow chart for calculation of heat and diffusion fluxes with evaporative mass injection or suction.

with maximum deviation less than 3%. **Figure 8** shows the results of the correlation.

3.2 Evaporative mass injection or suction

Under evaporative mass injection conditions Eq. (11) requires that the surface mass efflux should satisfy the following condition:

$$\phi(\theta) = \frac{\mathscr{D}(\omega_s-\omega_\infty)}{2AU_\infty(1-\omega_s)} \cdot Sh_\theta(1-\omega_s) \tag{25}$$

This requires an additional iteration loop in calculation of the stream functions. **Figure 9** shows a flow chart for the calculation. The following convergence criterion:

$$|C(\theta)/\bar{C}-1| < 0.001 \tag{26}$$

where

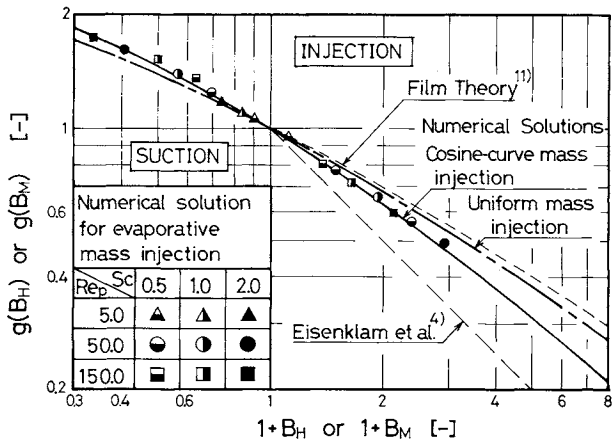

Fig. 10. Comparison of numerical data on evaporative mass injection or suction with results of uniform and cosine-curve mass injection or suction.

$$C(\theta)=\phi(\theta)/Sh_\theta(1-\omega_s) \tag{27}$$

was used for the present calculation.

Since calculation with evaporative mass injection requires a large computation time, usually 6 to 10 times that for uniform or cosine-curve mass injection, calculations were made only for a few examples.

Figure 10 shows a comparison of numerical results for evaporative mass injection with that for uniform (Eq. (22)) and cosine-curve (Eq. (24)) mass injection. The correlation for the cosine-curve mass injection showed good agreement with the numerical results for evaporative mass injection with maximum deviation less than a few percent. For the purpose of comparison, prediction by the simple film theory of mass injection over flat plate[11]:

$$g(B)=\ln(1+B)/B \tag{28}$$

and empirical correlation for a burning liquid drop by Eisenklam *et al.*[4]:

$$g(B)=1/(1+B) \tag{29}$$

are also shown in the figure. Good agreement of numerical results for evaporative and cosine-curve mass injection were observed between the two correlations. The reason for the large deviation of the Eisenklam correlation may be due to large scattering of their data and to uncertainties in B_H as discussed by Natarajan.[12]

Conclusions

Numerical analyses for heat and mass transfer of a solid sphere with and without mass injection or suction were made by use of a finite difference method for $Re_p=1$–200, Sc or $Pr=0.5$–2.0 and $\phi=-0.2$–0.5.

Heat and mass transfer of a solid sphere with and without mass injection or suction showed good agreement with the results of previous workers. Heat and mass transfer rates with mass injection or suction showed that the effect of mass injection or suction was affected by Re_p and Pr or Sc as well as mass injection ratio.

New correlations for the effect of mass injection or suction on heat and mass transfer of a solid sphere in terms of transfer numbers were proposed for the case with uniform and cosine-curve mass injection or suction. Heat and mass transfer with evaporative mass injection and suction showed good agreement with that for cosine-curve mass injection or suction.

Nomenclature

A	= radius of sphere	[m]
B_H	= transfer number for heat transfer, defined by Eq. (20)	[—]
B_M	= transfer number for mass transfer, defined by Eq. (21)	[—]
C	= parameter defined by Eq. (27)	[—]
c_p	= heat capacity at constant pressure	[J/(kg·K)]
$\mathscr{D}$	= diffusion coefficient	[m²/s]
E^2	= operator defined by Eq. (2)	[—]
g	= function defined by Eq. (18), (19); function of B	[—]
N_A	= mass flux of component A	[kg/(m²·s)]
Nu	= average Nusselt number, defined by Eq. (12)	[—]
Pr	= Prandtl number ($=\rho\nu c_p/\kappa$)	[—]
q	= heat flux	[W/m²]
r	= dimensionless radial distance ($=r'/A$)	[—]
Re_p	= Reynolds number ($=2AU_\infty/\nu$)	[—]
Sc	= Schmidt number ($=\nu/\mathscr{D}$)	[—]
Sh	= average Sherwood number, defined by Eq. (13)	[—]
t	= dimensionless time ($=U_\infty t'/A$)	[—]
T	= temperature	[K]
u_r	= dimensionless velocity in r direction ($=u_r'/U_\infty$)	[—]
U_∞	= free stream velocity	[m/s]
z	= dimensionless radial distance, defined by Eq. (5)	[—]
θ	= angle measured from forward stagnation point	[rad]
θ_c	= dimensionless concentration ($=(\omega_{As}-\omega_A)/(\omega_{As}-\omega_{A\infty})$)	[—]
θ_t	= dimensionless temperature ($=(T_s-T)/(T_s-T_\infty)$)	[—]
ν	= kinematic viscosity of gas	[m²/s]
κ	= gas-phase thermal conductivity	[W/(m·K)]
ρ	= density of gas	[kg/m³]
ϕ	= surface mass injection ratio ($=u_r'/U_{\infty\mid r=1}$)	[—]
$\phi(\theta)$	= local value of surface mass injection ratio, defined by Eq. (25)	[—]
ψ	= dimensionless stream function	[—]
ω_A	= mass fraction of component A	[—]

〈Subscripts〉

i	= mesh point in z direction
j	= mesh point in θ direction
0	= without surface mass injection or suction
s	= drop surface
θ	= θ direction; local value
∞	= free stream

⟨Superscripts⟩

k = number of iteration

$'$ = dimensional variables

$\bar{}$ = average with respect to θ

Literature Cited

1) Brauer, H. and D. Sucker: *Int. Chem. Eng.*, **18**, 375 (1978).
2) Chuchottaworn, P., A. Fujinami and K. Asano: *J. Chem. Eng. Japan*, **16**, 18 (1983).
3) Dennis, S. C. R., J. D. A. Walker and J. D. Hudson: *J. Fluid Mech.*, **60**, 273 (1973).
4) Eisenklam, P., S. A. Arunachalam and J. A. Weston: "Eleventh Symposium (International) on Combustion," pp. 715–727, Combustion Institute, Pittsburgh (1967).
5) Fujinami, A. and K. Asano: Proceeding of the 2nd International Conference on Liquid Atomization and Spray Systems, 13-2, 359 (1982).
6) Gal-Or, B. and D. Weihs: *Int. J. Heat Mass Transfer*, **15**, 2027 (1972).
7) Hamielec, A. E., T. W. Hoffman and L. L. Ross: *AIChE J.*, **13**, 212 (1967).
8) Hoffman, T. W. and L. L. Ross: *Int. J. Heat Mass Transfer*, **15**, 599 (1972).
9) Ikui, T. and M. Inoue: "Nensei Ryutai no Rikigaku," pp. 53–67, Rikogakusha, Tokyo (1979).
10) Masliyah, J. H. and N. Epstein: *Progr. Heat Mass Transfer*, **6**, 613 (1972).
11) Mickley, H. S., R. C. Ross, A. L. Squyers and W. E. Stewart: NACA TN 3208 (1954).
12) Natarajan, R.: *Combust. Flame*, **20**, 199 (1973).
13) Pruppacher, H. R. and R. Rasmussen: *J. Atmos. Sci.*, **36**, 1255 (1979).
14) Ranz, W. E. and W. R. Marshall: *Chem. Eng. Progr.*, **48**, 141 (1952).
15) Rowe, P. N., K. T. Claxton and J. B. Lewis: *Trans. Inst. Chem. Engrs. (London)*, **43**, T14 (1965).
16) Sayegh, N. N. and W. H. Gauvin: *AIChE J.*, **25**, 522 (1979).
17) Woo, S. E. and A. E. Hamielec: *J. Atmos. Sci.*, **28**, 1448 (1971).
18) Yuen, M. C. and L. W. Chen: *Int. J. Heat Mass Transfer*, **21**, 537 (1978).

(Presented at 16th Autumn Meeting of The Society of Chemical Engineers, Japan at Nagoya, October 1982.)

EXPERIMENTAL STUDY OF EVAPORATION OF A VOLATILE PENDANT DROP UNDER HIGH MASS FLUX CONDITIONS

PAILIN CHUCHOTTAWORN, AKIRA FUJINAMI AND KOICHI ASANO

Department of Chemical Engineering, Tokyo Institute of Technology, Tokyo 152

Key Words: Atomization, Mass Transfer, Heat Transfer, Evaporation, Pendant Drop, High Mass Flux, Transfer Number, Variable Property

Experimental studies on the rate of evaporation of a volatile, pendant liquid drop under high ambient temperature conditions (high mass flux) were carried out for the evaporation of water, methanol, *n*-hexane, *n*-pentane and carbon tetrachloride drops into dry air. Measurements were made for $Re_p = 32$–328, $Sc = 0.60$–1.66 and dimensionless driving force $B = 0.02$–1.36.

Experimental results for the rate of evaporation of a liquid drop under low ambient temperature conditions showed good agreement with the low-flux equation by Ranz and Marshall and also with previous numerical solutions. Experimental results for rate of evaporation under high ambient temperature conditions showed a systematic deviation from the Ranz–Marshall correlation.

Taking into account the effect of high mass flux together with the effect of variable properties, a new correlation equation was proposed which correlated all the experimental data very well.

Introduction

Evaporation of a volatile liquid droplet at high ambient temperatures is important in studies of the combustion of liquid fuel, quenching of hot gas and spray drying. Under such severe conditions surface mass efflux caused by diffusion of evaporating materials becomes so large that it will affect velocity, temperature and concentration fields around an evaporating drop and so-called high mass flux effect will take place. Under such conditions heat and mass transfer fluxes are quite different from those under low mass flux conditions or at low ambient temperatures.

Received January 8, 1983. Correspondence concerning this article should be addressed to K. Asano. A. Fujinami is now at Asahi Glass Co., Ltd., Chiba 273.